

Article

Application of D-Decomposition Technique to Selection of Controller Parameters for a Two-Mass Drive System

Radosław Nalepa ¹, Karol Najdek ¹, Karol Wróbel ²  and Krzysztof Szabat ^{2,*}

¹ Department of Electrical Power Engineering, Wrocław University of Science and Technology, PL50370 Wrocław, Poland; radoslaw.nalepa@pwr.edu.pl (R.N.); karol.najdek@pwr.edu.pl (K.N.)

² Department of Electrical Machines, Drives and Measurements, Wrocław University of Science and Technology, PL50370 Wrocław, Poland; karol.wrobel@pwr.edu.pl

* Correspondence: krzysztof.szabat@pwr.edu.pl

Received: 11 November 2020; Accepted: 10 December 2020; Published: 15 December 2020



Abstract: In this work, issues related to the application of the D-decomposition technique to selection of the controller parameters for a drive system with flexibility are presented. In the introduction the commonly used control structures dedicated to two-mass drive systems are described. Then the mathematical model as well as control structure are introduced. The considered structure has only basic feedbacks from the motor speed and PI type controller. Due to the order of the closed-loop system, the free location of the system's poles is not possible. Large oscillations can be expected in responses of the plant. In order to improve the characteristics of the drive, the tuning methodology based on the D-decomposition technique is proposed. The initial working point is selected using an analytical formula. Then the value of controller proportional gain is decreasing, until the required value of overshoot is obtained. In the paper different advantages of the D-decomposition technique are presented, for instance calculation of global stability area for the selected gain and phase margin, the impact of parameter changes, and additional delay evident in the system. Theoretical considerations are confirmed by simulation and experimental results.

Keywords: electric drives; two-mass system; torsional vibrations; D-decomposition

1. Introduction

At present, high precision control is required in most modern industrial processes [1–5]. Industrial automation is mainly based on the electrical servo systems with different types of driving motors. In order to ensure accurate control of servo, all factors which can affect the characteristic of the drive should be taken into account [1–5]. The mechanical characteristics of the system determine the performance of the speed/position control. The commonly-used approach, in which the mechanical shaft has an infinite stiffness coefficient, is not valid in many applications. As traditional examples rolling-mill drives or conveyer drives can be quoted [6–11]. In these applications large inertias and mechanical connections are evident. During transients the speed/position of the driving motor is different from the speed/position of the load side. The existing torsional vibrations influence the control performance significantly. Due to the progress of microprocessor technique and power electronics, which allows to generate the electromagnetic torque with a very small delay, nowadays this problem is also evident in different drive applications [7–11]. Torsional vibrations are recognised in servo systems, robot arm drives, CNC machines, hard disc drives, MEMS (micro electromechanical systems) [12–19], as well as in different industrial branches [20–23].

Different control strategies are proposed in literature in order to damp torsional vibrations [1–7]. The use of designated control strategies is one of the most effective and commonly used. The classical

control structure of an electrical motor has two major control loops. The electromagnetic torque is controlled in an inner loop effectively, using one of the well-established control strategies (current controller for DC drive, FOC, DTC or predictive for AC drives) based on the current(s)/voltage(s) sensor(s). The electromagnetic torque follows the reference value generated in an outer loop. The control problem of the mechanical part, including torsional vibrations, is evident in the outer speed control loop. In industrial drives usually one speed sensor fixed to driving motor is available. The basic control structure for the electrical drive has a classical PI controller usually tuned with the help of symmetric criterion. However, this approach is not effective enough, and can lead to big oscillation of the system states.

In order to increase the performance of the closed loop control structure different methods of selecting controller parameters have been proposed in the literature. In [6] a solution based on poles-placement methodology is proposed. Because the system is of the fourth order and there are only two design parameters (gains of PI controller), free selection of the location of system poles is not possible. Due to this reason, the authors proposed location of the circle (with identical value of the resonant frequency), on the line (with identical value of the damping coefficient) or alternatively with the same value of the real parts. These approaches reduce the overshoots of speed in the system, yet the performance improvement of the drive is limited.

A similar approach to this problem is presented in [7]. In this paper the relationship between individual closed-loop poles is shown. The author assumed the direct assignment of the dominant pair of poles, the position of second pair result from design requirements and limitations. This extends the possible location of poles presented in [6] and naturally extends possibilities of shaping the performance of the drive. However, it should be stressed that not all closed-loop poles locations are possible.

In order to damp torsional vibrations effectively, a more advanced approach is required. A commonly used solution is based on the insertion of additional feedbacks from one or more system state variables to the classical control structure—see survey paper for details [8]. The use of additional signals allows to damp torsional vibrations successfully. The drawback of this approach is the complicated control structure and difficulties in tuning of the control structure parameters.

In literature different control concepts for the drive system with flexibility are presented. Control systems with disturbance observer are among the most popular [1–5]. They allow to damp torsional vibrations and do not require large computational power. In [9] the FDC (forced dynamic control) methodology is proposed. The control structure allows to locate the system poles in a desired position and additionally has the ability to reject the effect of the load torque from the load side speed. The next approach is based on state controller methodology. Torsional vibrations are suppressed successfully in this structure. For high frequency oscillations, implementing digital filters is a well-established solution [24–32].

In the case of systems with parameter uncertainty or special requirements, more advanced control methodologies can be applied. The adaptive control structure, sliding-mode control structure, model predictive control structure and others can be implemented [23–30]. Although they ensure very good control characteristics, their main drawback is a complicated structure. Usually, information about the system state variables and parameters is required, so there is a need to implement a special estimation system (based on the Luenberger observer, Kalman filters, moving horizon estimator, neural networks etc. [24–27]), which further complicates the control algorithm and limits their application in industry.

The adaptive control structures can be divided into main two frameworks. In the first approach the so-called direct adaptive control is included. It is illustrated in paper [23], where MRAS (Model Adaptive Reference System) is proposed. This model represents the desired dynamics of the plant. Then the tracking error is calculated as the difference between outputs of the reference model and the object. Next, the parameters of the controller are retuned on the basis of the tracking errors and adaptation law in the way that minimises the difference between the model and plant outputs. In paper [23] two speed controllers are tested, namely the fuzzy-PI and fuzzy-sliding-mode. It was shown that

the fuzzy-sliding-mode controller can ensure much better performance of the drive in the case of parameter changes.

A similar concept is proposed in [28], where the ANFIS network is implemented as a speed controller. In the indirect adaptive frameworks the application of the special system (usually observers) which identifies (estimates) the changes of the system parameter(s) is necessary. Then, based on the current values of estimated parameter(s) and specify model, the new gains of the control structure are calculated and updated. In the paper [26] the adaptive control structure with PI controller and additional parameters are proposed. As an estimator the unscented Kalman filter is applied. The changeable value of time constant of the load machine is estimated. Then, with the help of specify formulas new coefficient are calculated and its value updated in the control structure. The application of this concept allows to keep the location of the system closed-loop poles in a desired position.

As drawbacks of the solution, the following issues should be mentioned. Firstly, the stability of the used estimator has to be guaranteed. The improper estimated values of the system parameters can disturb work of the control structure, even leads to instability. Secondly, the design of the estimator is not trivial task in every case. Thirdly, what is very important in industry, there is a need to have some computational power during implementation. This is problematic in standard industrial devices which often allow only to change controller parameters.

In industry more than 90% of all control structures are based on the simple PI/PID approach. In the area of the electrical drives, two specific criteria are especially popular, namely circle and modulus frameworks. However, in some specific cases (as the two-mass drive system considered here) the classical methodologies are not effective enough. Additionally, the solutions proposed in the literature [6,7] have some limitations. Therefore, further development of the algorithms which can improve the control system performances working with simple PI controllers are expected from industrial engineers. This is one of the motivations for this work.

The D-decomposition algorithm was proposed by Yuri Isaakovich Neimark [33]. With the use of this methodology asymptotically stable regions as a function of the system parameters can be calculated. The original form of the algorithm exhibits many shortcomings, which limit its application in science and industries. The main drawback is again a complicated mathematical algorithm. Due to the progress of computational power of computer systems this is no longer a limiting factor. Over a period of time, the D-decomposition technique has been modified and improved [34–38]. For instance, it can take into account constraints such as gain and phase margins [39], yet works showing applications of the D-decomposition technique to the mechatronic system are rare in the literature.

In this paper the issues related to the D-decomposition technique to selection of the controller parameters of the industrial drive with elasticity are presented. The classical control structure of an electrical drive including two major loops (torque, speed) is considered. The inner loop is assumed to be optimized and provide sufficiently fast torque responses. In the speed loop the classical PI speed controller is applied. In the previous work [39] the poles-placement methodologies were presented and its limitations were pointed out. Additionally, the D-decomposition technique was introduced and generally described. Then the preliminary simulation and experimental transients were submitted and discussed. The proposed methodology allows to select the controller's parameter taking into account different factors, for instance the assumed gain and phase margin. In the present research the description of D-decomposition technique is specified. The presented equations are specified for the considered case—a two-mass drive system with delays. So, the effect of the delays evident in the control structure is included into considerations. As a result, the D-decomposition provides regions in which the specified conditions are fulfilled. Further, this algorithm can be also used to analyse the effect of changes of parameters on the closed-loop stability. The theoretical consideration are confirmed by a number of simulation as well as experimental studies. At the end of the paper, concluding remarks are formulated.

The paper consists of five sections. In the introduction motivation for the work is explained. A short survey of the control structures designated for two-mass drive systems is presented. Then, the model of

the drive system with a flexible connection is introduced briefly. The commonly used control structure for an electrical drive is described in details. The application of poles-placement methodologies to the selection of controller parameters is shown. The limitations of the classical control design methodology are emphasized. In the third section the D-decomposition technique is presented. Next, the application of the D-decomposition technique to selection of controller parameters is discussed. Different design factors, such as: phase margin, gain margin, delay times, changes of the system parameters are considered. Additionally, the stability issues are considered. Next, the selected experimental results are presented and discussed. The concluding remarks are formulated at the end of the paper.

2. Mathematical Model of the Plant and Control Structures

In order to analyze the plant there is a need of selection of a suitable mathematical model. In general, two groups of modeling can be distinguished in mechatronic systems. The first one is based on the finite element method. This approach allows to analyse the whole system very thoroughly, yet computational complexity is very high. This modeling is very popular, for example in designing electrical machines. The second modeling approach is based directly on differential equations. It allows to determine the behavior of the system vary fast, so it is popular in control engineering. However, the accuracy of obtained results is limited. The selection of one of the above-mentioned models usually depends on the application. In implementations for which time is crucial (real time control), only the second modeling approach is possible.

In the work, a commonly applied model of the drive system with flexible connection (two-mass system) is used. It is based on three differential equations, which describe the behavior of the three states of the system. This state equation representing the model is presented below [6,8]:

$$\frac{d}{dt} \begin{bmatrix} \omega_1(t) \\ \omega_2(t) \\ m_s(t) \end{bmatrix} = \begin{bmatrix} 0 & 0 & \frac{-1}{T_1} \\ 0 & 0 & \frac{1}{T_2} \\ \frac{1}{T_c} & \frac{-1}{T_c} & 0 \end{bmatrix} \begin{bmatrix} \omega_1(t) \\ \omega_2(t) \\ m_s(t) \end{bmatrix} + \begin{bmatrix} \frac{1}{T_1} \\ 0 \\ 0 \end{bmatrix} [m_e] + \begin{bmatrix} 0 \\ \frac{-1}{T_2} \\ 0 \end{bmatrix} [m_L] \quad (1)$$

where: ω_1, ω_2 —the speeds of driving motor and load machine respectively, m_e, m_s, m_L —the electromagnetic (driving), shaft (coupling), and load torques, T_1, T_2 —mechanical time constant of the driving motor and load machine, T_c —the parameter which represents the elasticity of the coupling.

The block diagram of the considered plant is shown in Figure 1.

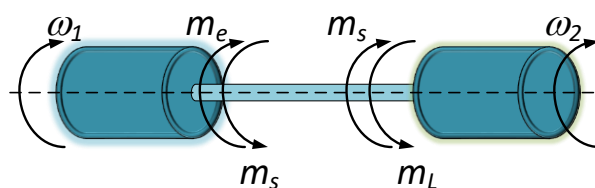


Figure 1. Block diagram of the two-mass system.

The electromagnetic torque is an input variable in that system. It is compared with the shaft torque (which can be treated as a load torque here and in normal condition has zero value at start) and the difference is accelerating the first mass. The mechanical time constant is proportional to the inertia of the driving motor. The changes of motor speed result in changing of its position, which causes the twist of the shaft. This, in turn, generates a non-zero value of shaft torque which with some delay is acting on the second inertia. The second speed is calculated as integration of the difference between the shaft and the load torque. During transients both speeds can have different values.

In industry, a standard control structure for an electrical drive has the following form. It is based on the two main control loops [8]. The inner loop provides the control of the electromagnetic torque. It can have different forms resulting from the type of the driving motor. In the case of a DC motor it is based on an armature current controller. For induction or PMSM motor the DFOC

(direct field oriented control) or DTC (direct torque control) is a standard solution. The task for the inner loop is to follow the reference value of torque relatively fast. The outer loop in the electrical drive encompasses the mechanical part of the drive. The main task for this loop is to control the system speed. The standard drive has only one feedback from the motor speed, and this signal is used for control. The speed PI controller evident here is tuned usually by symmetry criterion. In the case of a stiff mechanical connection, this feedback can ensure accurate control. However, in the case of a flexible connection there is a possibility to introduce torsional vibrations into the system. As it is mentioned in the introduction, there are many different control structures which can be used to suppress torsional vibrations. The most advanced ones are based on the additional feedbacks from all state variables of the plant (motor speed, shaft torque, load speed and in some cases the load torque). This allows to damp the torsional vibrations successfully. The drawback of these approaches is a complicated control algorithms—this limits the application of such structures in industry. One of the possible solutions, which does not influence the form of the control structure, is changing the methodology used for selection of the parameters of the speed controller.

In the paper the classical control structure with basic feedback from the motor speed is considered (Figure 2).

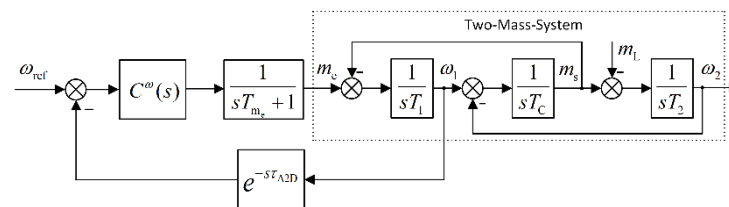


Figure 2. A block diagram of the considered control structure.

In the block diagram presented in Figure 2, two control loops are evident. The inner, torque control loop, is approximated by first order term with small time constant (T_{m_e}). Because this time is much smaller than time constants evident in the mechanical part of the drive, it is usually neglected in analysis. The outer loop encompasses the following elements: the mechanical part of the driving motor, shaft, load machine, speed sensor and speed controller ($C^\omega(s)$). Additional delays caused by the speed sensor, sampling time in processor are also often neglected (represented in Figure 2 by following element $e^{-sT_{A2D}}$). This element represents delays caused by the sensor itself (which usually is small) and by sampling time of speed loop. In the D-decomposition technique all these delays can be taken into account in a natural way.

In order to show the advantages of the D-decomposition technique, design process with the help of classical poles-placement is introduced [6,7]. It is based on the following procedure.

Firstly, closed-loop transfer functions from the reference signal to the speed of load machine are calculated (assuming that all delays in the system are neglected):

$$G(s) = \frac{\omega_2(s)}{\omega_z(s)} = \frac{G_r}{s^3 T_1 T_2 T_c + s^2 T_2 T_c G_r + s(T_1 + T_2) + G_r} \quad (2)$$

where G_r —PI controller transfer function.

Then the characteristic equation of the system given by:

$$s^4 + s^3 \left(\frac{K_P}{T_1} \right) + s^2 \left(\frac{K_I}{T_1} + \frac{1}{T_1 T_c} + \frac{1}{T_2 T_c} \right) + s \left(\frac{K_P}{T_1 T_2 T_c} \right) + \frac{K_I}{T_1 T_2 T_c} = 0 \quad (3)$$

is compared to the desired polynomial which has following form:

$$(s^2 + 2\xi\omega_0 s + \omega_0^2)(s^2 + 2\xi\omega_0 s + \omega_0^2) = 0 \quad (4)$$

where: ξ —damping coefficient, ω_0 —resonant frequency of the closed-loop system.

After multiplication, the Equation (10) can be rewritten as follows:

$$s^4 + s^3(4\xi\omega_0) + s^2(2\omega_0^2 + 4\xi^2\omega_0^2) + s(4\xi\omega_0^3) + \omega_0^4 = 0 \quad (5)$$

Comparing Equations (3) with (5), the set of four equations is created. Finally the equations which allow to set the controller parameter are obtained.

$$K_P = 2\sqrt{\frac{T_1}{T_c}}, \quad K_I = \frac{T_1}{T_2 T_c} \quad (6)$$

The following remarks can be formulated through the analysis of Equation (6). The gains of the controller depend on the particular parameter of the plant. It means that the system closed-loop poles cannot be located freely in an imaginary plane. It results from the fact that there are four poles of the closed-loop system (three poles from the plant and one from the controller) and there are only two design parameters. Equation (6) ensures double location of the closed-loop poles.

In order to demonstrate the properties of the system with proposed approach the simulation study are performed. The system with two value of inertia ratio $R = T_2/T_1$ is considered, namely $R = 1$, $R = 0.5$. The system is working with the following cycle. At the time $t_1 = 0$ s the reference value of the speed is set to 0.2. Then at the time $t_2 = 0.4$ s the nominal torque is applied to the system. Finally, the load torque is switched off at $t_3 = 0.6$ s. The obtained transients of the system speeds and torques are presented in Figure 3.

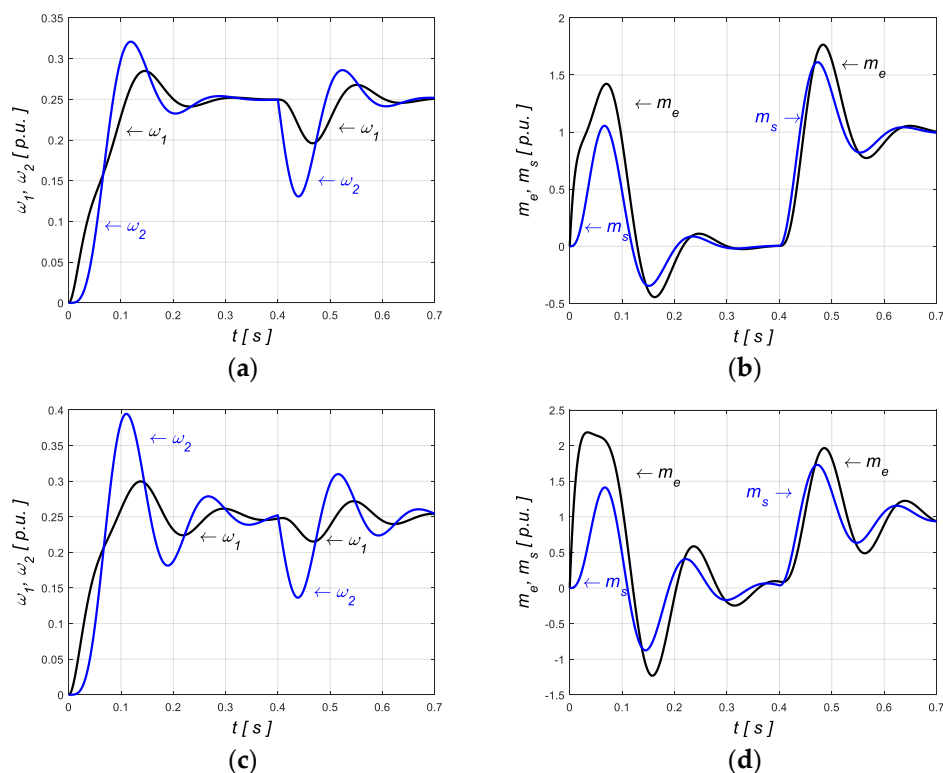


Figure 3. Transients of the two-mass system: motor and load speed (a,c), electromagnetic and shaft torque (b,d) for different value of the inertia ratio coefficients $R = 1$ (a,b) and $R = 0.5$ (c,d).

The following remarks can be formulated from the transients presented in Figure 3. The overshoot in the system speeds depends strictly on inertia ratio. For a small value of R , in the system speeds there are large overshoots and oscillations. These oscillations decrease as R increase. However, the raising

time of the system in case of bigger value of R also increased. Those oscillations are also visible in transients of driving and shaft torques.

Because oscillations in system state transients are not acceptable in modern drives, different tuning methodologies of the PI controller are looking for. In the [6] possibility of location of system closed-loop poles on the circle, line with identical damping coefficient and line with equal real part has been proposed. The more detailed studies concerning the influence of alternative closed-loop poles location to drive performances are presented in [7]. This alternative closed-loop poles location improve system performances, yet only in some limited range. Additionally, the effect of additional delays and parameter changes are not included in classical poles-placement methodology. Therefore, other tuning criteria are sought after. In this paper the D-decomposition methodology, presented in the next section, is proposed.

3. D-Decomposition Technique

Relationship between frequency domain criterion (phase and gain) and of the n^{th} -order characteristic equation, and a space of permissible parameters for which the stability condition is met can be established by means of the D-decomposition technique.

Boundary of the stable region can be calculated by substituting $s = j\omega$ in the characteristic equation, where the pulsation ω is to be understood as a real number in range $-\infty < \omega < +\infty$. As next, the real and imaginary parts of obtained expression must be equated to zero. By solving such equations one can reach dependencies describing parametric hypersurface which designates the stability boundary in the so called D surface. The D surface, as a parametric surface $D(l, r = n - l)$, relies on l and r standing for number of the characteristic equation roots in the left and right half-plane, respectively. There are no roots in the right half-plane, $r = 0$ if $l = n$. In such condition the designated surface $D(l = n, 0)$ indicates a stable region [34]. Once the stability boundary is known, it is necessary to indicate the stable side. For a single parameter, the left-hand side of the boundary is the stable region, where left-hand side is referred to drawing the boundary by changing frequency in direction from $-\infty$ to $+\infty$. For two tuneable parameters an additional boundary is needed. It is so called ΔD_0 hyperplane [34]. It is designated by comparison of the characteristic equation to 0 at the origin of the s -plane, $s = 0$. Solution leads to a complementary criterion for the second parameter region.

By introducing additional Gain Margin (GM), and Phase Margin (PM), criteria an internal boundary must be found within the asymptotic stability region. This can be realized by equating the characteristic equation to a complex number instead of zero. The complex number represents the required GM and PM.

A well-known expression for the closed-loop transfer function of a standard control structure can be written as:

$$G_{CL}(s) = \frac{Y(s)}{R(s)} = \frac{C(s)P(s)}{1 + C(s)P(s)} \quad (7)$$

where: $C(s)$ —the regulator transfer function; $P(s)$ —controlled plant transfer function; $R(s)$ —reference signal; $Y(s)$ —the plant output. One should notice, that the $1 + C(s)P(s) = 0$ represents the characteristic equation. The $C(s)P(s)$ part stands for the open loop transfer function, $G_{OL}(s)$. For being more specific, assume a 3rd-order plant transfer function as shown in Figure 2:

$$P(s) = \frac{\omega_2(s)}{m_e(s)} = \frac{1}{s^3(T_1 T_2 T_C) + s(T_1 + T_2)} \quad (8)$$

where: T_1 is the mechanical time constant of the motor; T_2 is the mechanical time constant of the load; T_C is the mechanical time constant of the shaft.

In such cases Equation (7), with assumed IP regulator, can be rewritten:

$$G_{CL}(s) = \frac{K_I}{s^4 + s^3\left(\frac{K_P}{T_1}\right) + s^2\left(\frac{K_I}{T_1} + \frac{1}{T_1 T_C} + \frac{1}{T_1 T_2 T_C}\right) + s\left(\frac{K_P}{T_1 T_2 T_C}\right) + \left(\frac{K_I}{T_1 T_2 T_C}\right)} \quad (9)$$

where: K_I is the integral gain; K_P is the proportional gain. The denominator of (9) is the characteristic equation with the -1 comprised inside.

In general, the characteristic equation in the frequency domain, $s = j\omega$, can be written as following:

$$G_{OL}(j\omega, K_P, K_I) = -1 + j0 \quad (10)$$

The equation can be rewritten as:

$$\Re[G_{OL}(j\omega, K_P, K_I)] = -1 \quad (11)$$

$$\Im[G_{OL}(j\omega, K_P, K_I)] = 0 \quad (12)$$

Solving the (11) and (12) for the K_P and K_I leads to:

$$K_P(\omega) = 0, K_I(\omega) = \omega^2 \left(T_1 + \frac{T_2}{1 - T_2 T_C \omega^2} \right) \quad (13)$$

Additionally, the ΔD_0 hyperplane boundary is:

$$\Delta D_0 \Rightarrow K_I = 0 \quad (14)$$

The Equations (13) and (14) are describing the parametric hypersurface designating the stability boundary on the D surface. Nevertheless, they do not take into account the reality in form of the system delays, e.g., the signal conversion delay, τ_{A2D} , as shown in (3).

When τ_{A2D} time delay is taken into account, the block diagram shown in Figure 2 leads to the closed loop transfer function written as:

$$G_{CL}(s) = \frac{K_I}{s^5 A_1 + s^4 A_2 + s^3 A_3 + s^2 A_4 + s^1 A_5 + A_6} \quad (15)$$

where, for equation simplicity reasons:

$$A_1 = T_1 T_2 T_C T_{me} \quad (16)$$

$$A_2 = T_1 T_2 T_C \quad (17)$$

$$A_3 = e^{-s\tau_{A2D}} K_P T_2 T_C + T_1 T_{me} + T_2 T_{me} \quad (18)$$

$$A_4 = T_1 + T_2 + e^{-s\tau_{A2D}} K_I T_2 T_C \quad (19)$$

$$A_5 = e^{-s\tau_{A2D}} K_P \quad (20)$$

$$A_6 = e^{-s\tau_{A2D}} K_I \quad (21)$$

Additionally, the T_{me} represents time constant of an electromagnetic torque control loop and $C^\omega(s)$ represents transfer function of the speed compensator.

Following the same procedure as above, the K_P and K_I can be found as functions of ω :

$$K_P(\omega) = \frac{\omega(T_1(T_2 T_C \omega^2 - 1) - T_2)(T_{me} \omega \cos(\tau_{A2D} \omega) + \sin(\tau_{A2D} \omega))}{T_2 T_C \omega^2 - 1} \quad (22)$$

$$K_I(\omega) = \frac{\omega^2(T_1(T_2 T_C \omega^2 - 1) - T_2)(T_{me} \omega \sin(\tau_{A2D} \omega) - \cos(\tau_{A2D} \omega))}{T_2 T_C \omega^2 - 1} \quad (23)$$

Now, for certain gain and phase margins, GM and PM , the open loop transfer function must be evaluated as:

$$G_{OL}(j\omega, K_P, K_I) = a + jb \quad (24)$$

where the $a + jb$ stands for coordinates of an arbitrary point in the polar plane. In such conditions the K_P and K_I gains for required GM in dB can be written as:

$$K_P(\omega, GM) = \frac{\omega(-T_2 + T_1(-1 + T_2 T_C \omega^2))(T_{me} \omega \cos[\omega T_{A2D}] + \sin[\omega T_{A2D}])}{-1 + T_2 T_C \omega^2} \quad (25)$$

$$K_I(\omega, GM) = -\frac{1 - 10^{\frac{-GM}{20}} + \omega^2(T_1 + T_2 - T_1 T_2 T_C \omega^2) \cos[\omega T_{A2D}] + T_{me} \omega^3(-T_1 - T_2 + T_1 T_2 T_C \omega^2) \sin[\omega T_{A2D}]}{-1 + T_2 T_C \omega^2} \quad (26)$$

Similarly, for the PM in degrees the K_P and K_I are:

$$K_P(\omega, PM) = \frac{T_{me} \omega^3(-T_2 + T_1(-1 + T_2 T_C \omega^2)) \cos[\omega T_{A2D}] + \sin[\frac{\pi PM}{180}] + \omega^2(-T_1 - T_2 + T_1 T_2 T_C \omega^2) \sin \omega T_{A2D}}{\omega(-1 + T_2 T_C \omega^2)} \quad (27)$$

$$K_I(\omega, PM) = \frac{-1 + \cos[\frac{\pi PM}{180}] + \omega^2(-T_1 - T_2 + T_1 T_2 T_C \omega^2) \cos[\omega T_{A2D}] + T_1 T_{me} \omega^3 \sin[\omega T_{A2D}]}{-1 + T_2 T_C \omega^2} + \frac{T_2 T_{me} \omega^3 \sin[\omega T_{A2D}] - T_1 T_2 T_C T_{me} \omega^5 \sin[\omega T_{A2D}]}{-1 + T_2 T_C \omega^2} \quad (28)$$

In terms of qualitative visualization, the Equations (25)–(28) together with (22) and (23), and the $\Delta D_0 = 0$ lead to trajectories as shown in Figure 4. The intersection point between GM and PM lines stands for our desired gains fulfilling the GM and PM conditions.

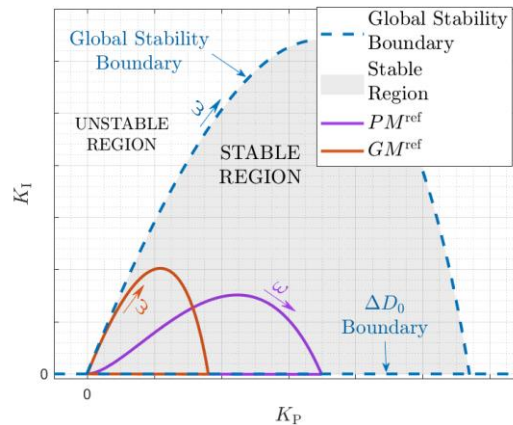
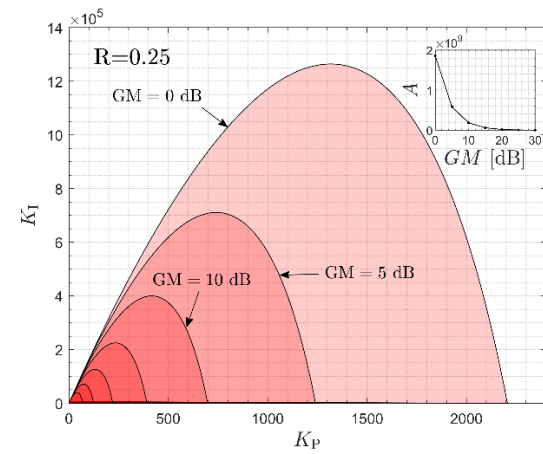


Figure 4. Qualitative visualization of the global stability boundary together with the boundaries for the desired PM and GM for control structure shown in Figure 2. The intersection of the PM and GM lines stands for the requested dynamics.

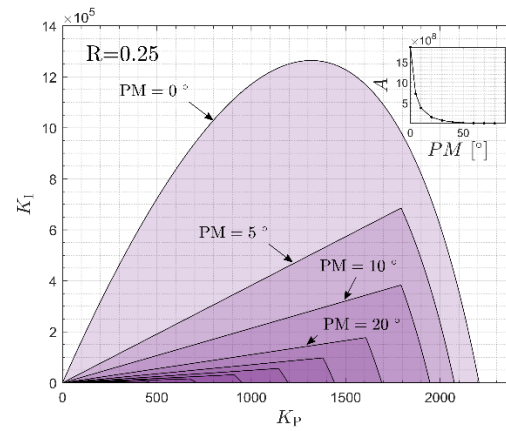
4. Results

In this section the simulation and selected experimental results concerning the application of the D-decomposition technique are presented. According to the description included in the previous section, the proposed methodology allows to determinate the controller parameters taking into account different factors, such as gain margin, phase margin, additional delay. Additionally, the effect of the changes of the plant parameters can be analysed using the D-decomposition technique. All these cases are presented below. The system with two inertia ratio value is considered: $R = 1$ and $R = 0.25$.

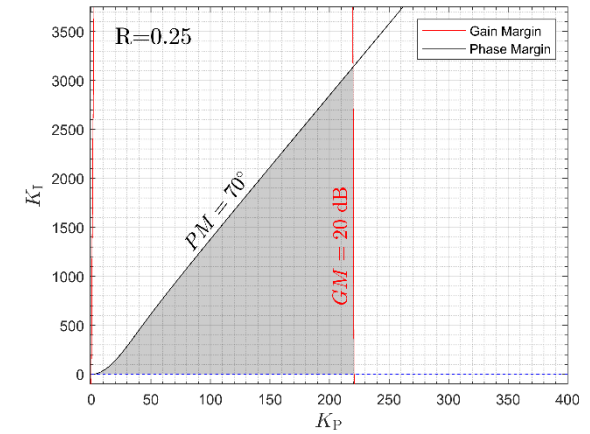
Firstly, the general properties of the D-decomposition technique are shown. The algorithm allows to calculate the stability region of the controller for hypothetical parameters of the plant ($T_1 = 812$ ms, $T_2 = 203$ ms, $T_c = 2.6$ ms for $R = 0.25$ and $T_1 = T_2 = 203$ ms, $T_c = 2.6$ ms for $R = 1$ and additional delays $T_{me} = 0.1$ ms, $\tau_{A2D} = 0.5$ ms). In Figure 5 the graphical illustration of the stability region of the control structure for different value of the gain margin and phase margin are presented.



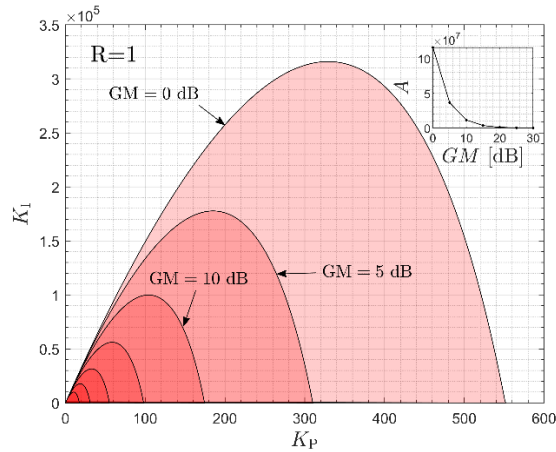
(a)



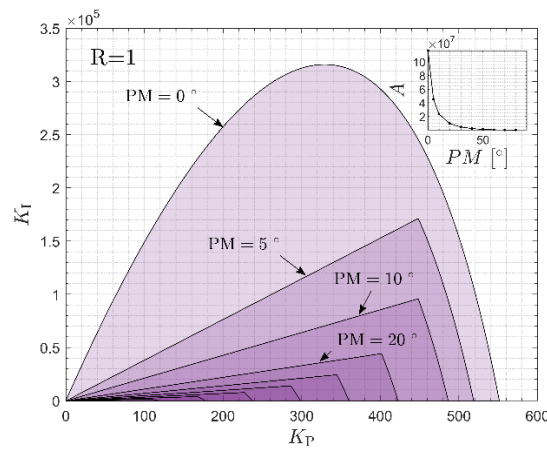
(b)



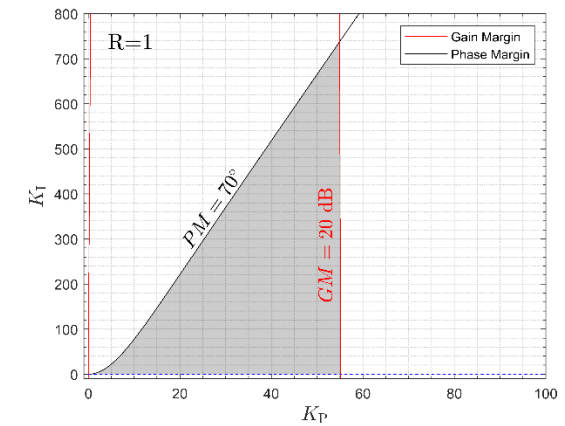
(c)



(d)



(e)



(f)

Figure 5. Visualisation of the desired regions for different value of the gain margin, GM , (a,d), phase margin, PM , (b,e) as well as selected value of $GM = 20$ dB and $PM = 70^\circ$ (c,f) for the control structure from Figure 2 and value of inertia ratio $R = 0.25$ (a–c) and $R = 1$ (d–f) calculated using D-decomposition technique. Results were obtained for $T_{m_e} = 0.1$ ms and $\tau_{A2D} = 0.5$ ms. Additionally, the total area, A , of obtained regions were presented.

As can be concluded from the presented graphs, the D-decomposition technique allows to determine the stable regions (relationship between the gains of the controller) of the system. The bigger area is calculated for the zero value of the GM and PM. Increasing these values decreases the stable area. For example, setting value $PM = 80$ results in a very small area of the stable work. Usually, these two conditions are specified during design of the control structure. In Figure 5c,f, the solution is presented for $GM > 20$ dB and $PM > 70^\circ$. All pairs of the controller coefficients laying into the area limited by two curves fulfilled the condition. The crossing point indicates the exact value of the conditions $GM = 20$ dB and $PM = 70^\circ$. The characteristics PM and GM as a function of total area of region A are similar for two considered inertia ratios. They differ by values, not by shapes. Although the presented methodology simplifies the design of the control structure, by indicating of the stable region of the work and limiting the hypothetical gains of the controller for setting condition, the selection of the particular values required expertise in this field. Therefore, in the next paragraph the procedure is developed to simplify the tuning process.

The drive with following value of the inertia ratio $R = 0.25$ is considered at first. The results of application of D-decomposition technique is a plane representing the stability area as the function of the controller parameters (proportional and integration gains). The enlarged plot is shown in Figure 6a. The following remarks can be formulated based on the following figure. The stable region of the system work is relatively wide. There is a problem to specify optimal working point (pairs of K_I and K_P) at start because there is a lot of possible solutions. This is a problem for industrial engineers which are asking for a simple and reliable tuning procedure. Therefore, the starting point is selected with the Equation (6) coming from poles-placement methodology. This initial working point P_1 is indicated in Figure 6a by red circle. Then this point is shifted down keeping the constant value of the gain margin and increasing value of the phase margin until the transition point P_2 . The final point is marked with P_3 . In the considered case, the proportional gain is keeping at constant value when the integral gain is reduced from 750 to 450. In order to demonstrate the effectiveness of the proposed procedure transients of the state variables of the system, for different selected points (P_1 , P_2 , and P_3) are plotted in Figure 6d–f.

The system is working under the following cycle. At the time $t_1 = 0$ s the reference value of the speed is changing from 0 to 0.2 (the low value of the speed is used in order to avoid the electromagnetic torque limit). Then at the time $t_2 = 0.3$ s the nominal load torque is applied to the system. As can be concluded from the Figure 6, the drive system with the gains of the controller selected using classical methodologies (6) has big oscillations and slowly damped overshoots in all state variables. Changing the working point from P_1 , through P_2 and finally to P_3 results in decreasing oscillations in all state variables. The overshoot in load speed is reduced from almost 90% (P_1) through 40% (P_2) and in the final point to 8% (P_3). It should be stressed that the settling time of the system is the shortest for point P_3 . The changing of working point requires to decrease only K_I controller coefficient. This makes this procedure easy to perform without advanced knowledge of D-decomposition. However, it should be stressed that this methodology offers more possibilities which is going to be shown later.

In order to confirm the effectiveness of the proposed solutions, additional characteristics of the system are generated. The relationship between the overshoot of load speed and controller parameters (Figure 6b) as well as the values of ITAE (integral of time-weighted absolute error—Figure 6c) are shown. The considered working points of the system are also marked in both diagrams. This figure is generated in a program which is not a part of the D-decomposition technique. Using this additional figures the effectiveness of the proposed tuning methodology can be confirmed. Additionally, for this particular system different values of plant responses can be obtained. The following remarks can be formulated on the basis of the presented characteristic. The application of changing of operation point allows to improve the system performance significantly. The overshoot is reduced to a small value. The further increase of the phase margin can eliminate the overshoot completely, yet the settling time of the system will be longer. This is clearly visible in Figure 6c, where the value of ITAE is presented.

The point P_3 ensures quasi optimal solutions. The global optimum can be obtained by also decreasing slightly the integrational gain of the controller.

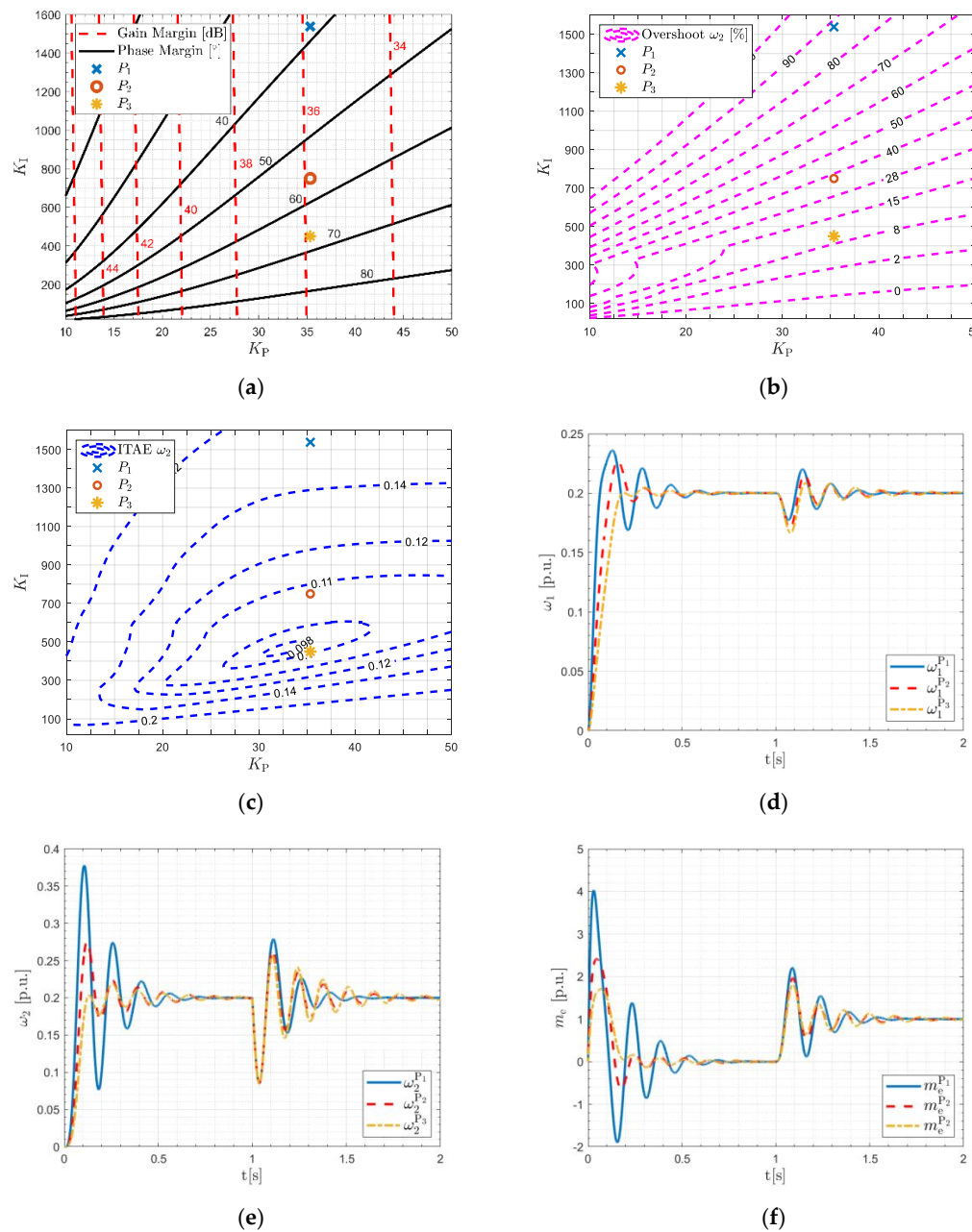


Figure 6. Characteristics of the system: stable region of work (a), overshoot in ω_2 (b), value of ITAE for ω_2 (c) transients of motor speed ω_1 (d), load speed ω_2 , (e) and shaft torque m_s (f).

Then the system with $R = 1$ is considered. The analogical characteristic and transients are plotted in Figure 7. The tuning procedure of the controller parameters is repeated once again. The D-decomposition technique is used to determine the plane where the stable region of work. Next, using (8) the initial working point is specified. Then the value of phase margin is reduced until the point P_3 is reached. It should be noted that for the system with $R = 1$ the reduction of K_I coefficient is smaller than in the previously considered case. The overshoot in load speed decreased from 28 to 2%.

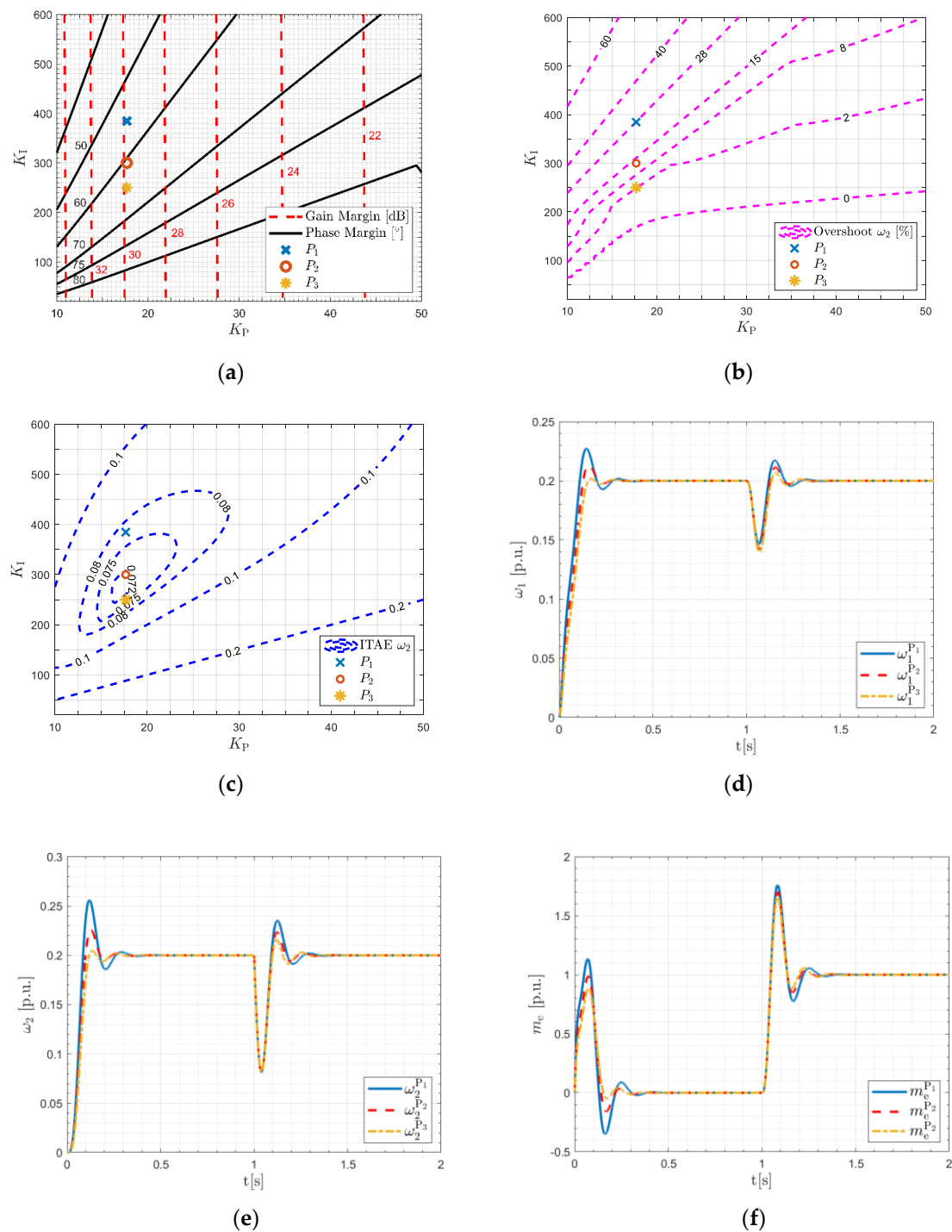


Figure 7. Characteristics of the system: stable region of work (a), overshoot in ω_2 (b), value of ITAE for ω_2 (c) transients of motor speed ω_1 (d), load speed ω_2 , (e) and shaft torque m_s (f).

The application of the above-described procedure result is improving characteristics of the system. The overshoot of both speeds are reduced as well as the settling time is shorten. The additional characteristics plotted in Figure 8b,c show the similar properties as in the previously considered case. The point P_3 is a quasi-optimal solution taking into account values of ITAE (Figure 7c).

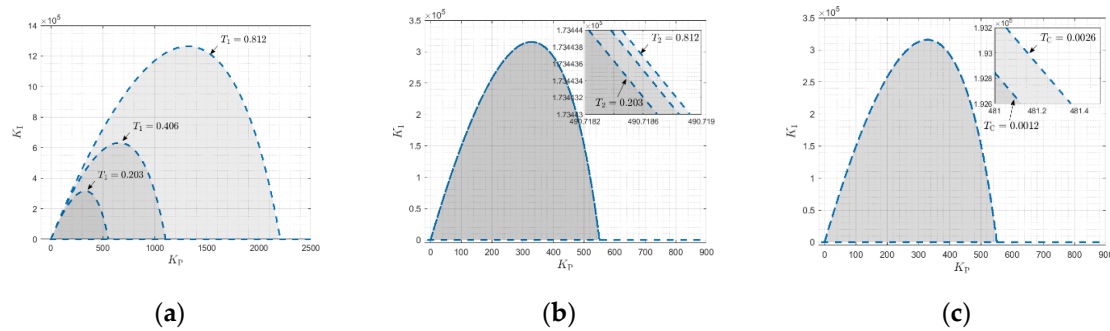


Figure 8. Global stability region of the control structure for different value of the plant's parameters: time constant of the driving motor (a), time constant of the load machine (b) as well as time constant of the elastic shaft (c).

In the case of the two-mass system with different parameters of the plant, two types of characteristics are commonly used. The simplest solution is based on the presentation of influence of particular parameters of the drive to selected property (here stability). The more advanced approach relies on presentation of the changes of inertia ratio R (or resonant frequency) to properties of the system [6,7]. Although the second framework is more generalised, it is less visible for wide group of engineers not specialist in considered problem. Taking into account these considerations, the first solution is implemented in this paper.

The D-decomposition technique can be also use to determinate the stable region of the control structure for different parameters of the plant. In Figure 9 the plots of the stable regions for different parameters of the plant are presented. The changes of the mechanical time constant of the motor T_1 (Figure 8a), changes of mechanical time constant of load machine T_2 (Figure 8b) and changes of elasticity time constant T_c (Figure 8c) are considered.

The following assertions can be specified of the basis on the Figure 8. The changes of time constant of the driving motor influence the stability region of the control structure significantly. The increase of T_1 enlarge stability region significantly. The value of proportional gains rise from 550 (for $T_1 = 203$ ms) to 2200 (for $T_1 = 812$ ms). Similarly, the maximal values of integral gains change from 3000 to 12,500. The changes of the two resting parameters T_2 and T_c have a much smaller impact to the stability regions (Figure 8b,c). Increasing these values hardly enlarges stability area of the controller.

The decomposition technique can be also used for analysing the impact of the delays evident in the control structure for the stability of the system. This is next investigated topic. First, the system with following parameters is tested: $GM = 20$ dB, $PM = 70^\circ$, $R = 1$ and two values of delay in torque control loop $T_{me} = 0.1$ ms (Figure 9a) and $T_{me} = 2$ ms (Figure 9b). The influence of delay τ_{A2D} to stability regions are presented in Figure 9b. Then the following case is considered. The delay in the converter is kept constant $\tau_{A2D} = 0.5$ ms (Figure 9c) and $\tau_{A2D} = 50$ μ s (Figure 9d) and the delay in the torque control loop T_{me} is variable (Figure 9c,d). The similar tests are repeated for the system with $R = 0.25$. The obtained results are presented in Figure 10.

The following remarks can be formulated on the basis on presented graphs (Figures 9 and 10). As can be expected the biggest regions are obtained for the system with minimal values of additional delays (Figures 9a,d and 10a,d). The increase of both delays narrow the stability region. The systems with minimal value of τ_{A2D} have the biggest stability area (Figures 9d and 10d), but when parameter T_{me} increases, the stability area is reduced significantly. In Figures 9b,c and 10b,c the characteristics for the system with parameters of used in the paper experimental set-up are presented. It is visible in total area A that the delay in torque control loop T_{me} has less impact on narrow the stability regions than delay τ_{A2D} . Comparing the shape of characteristics for different inertia ratio R , it can be concluded that they have similar features, only the scale of controller parameters are different.

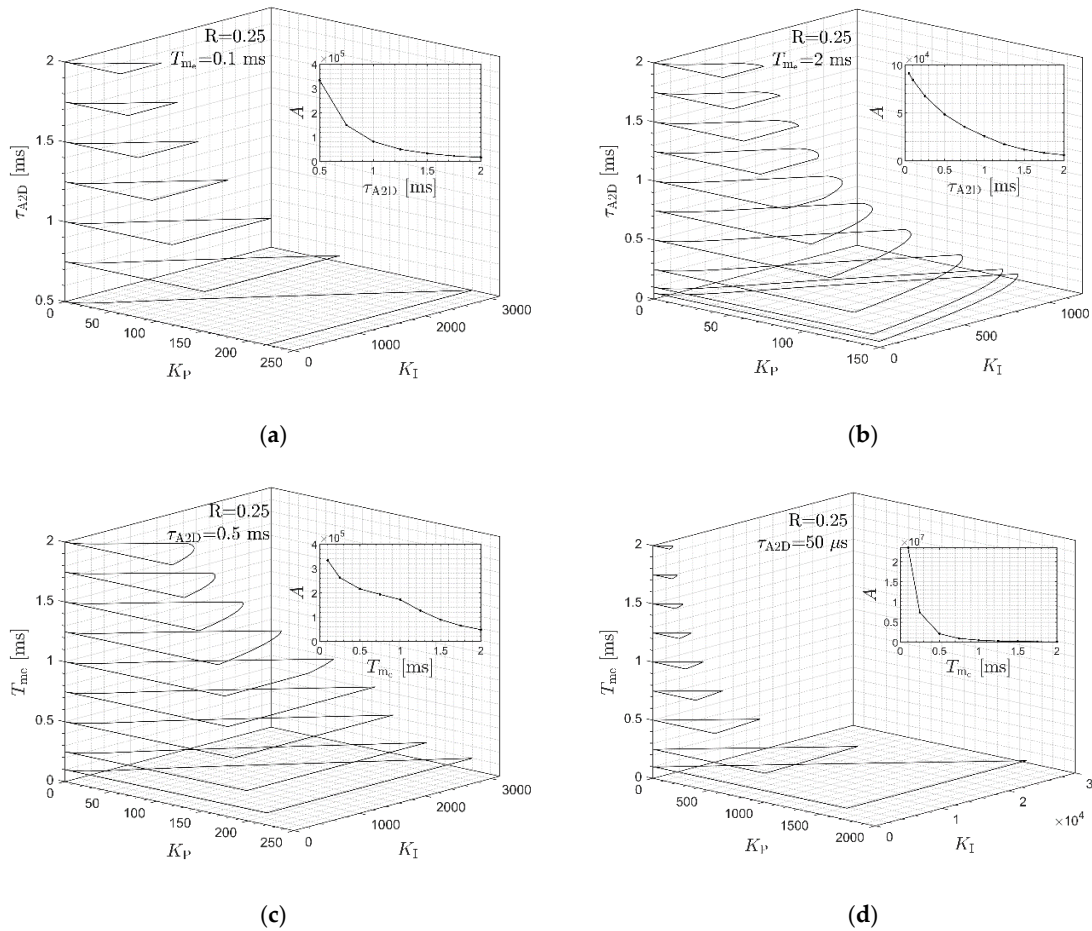


Figure 9. Visualisation of the K_P and K_I regions for desired values of $GM = 20$ dB and $PM = 70^\circ$ for the control structure from Figure 2 calculated using D-decomposition technique. Results were obtained for the value of inertia ratio $R = 0.25$, time constant of the elastic shaft, $T_C = 2.6$ ms, and value of electromagnetic torque time constant $T_{me} = 0.1$ ms (a) and $T_{me} = 2$ ms (b) and delay from analogue-to-digital conversion in the speed sensor $\tau_{A2D} = 0.5$ ms (c) and $\tau_{A2D} = 50$ μ s (d). Additionally, the total area, A , of obtained regions were presented.

The simulation results have been confirmed using a laboratory set-up. The main part of the laboratory stand consists of two DC motors connected by a long elastic shaft (made of steel with length 600 mm and 5 mm diameter). There are additional flywheels which allow to change the moment of inertia of motor and load machine. Both motors have a nominal power equal to 500 W. The driving motor is supplied by power converter (H bridge structure) which allows the flow of the armature current in both directions. The control of the load torque is obtained by switching on and off to armature winding to resistor. The speed of the motor and load machine is measured using incremental encoders (36,000 pulses per revolution). The control algorithm is implemented in real-time using dSpace control desk. The obtained sampling time is equal to 0.5 ms (including speed and torque loops). The picture of experimental ring is shown in Figure 11.

In the experimental tests the theoretical results have been confirmed. The system is working under the following cycle. At the time $t_0 = 0$ s the reference value is changing from 0 to 0.2 s. The initial value of load torque is set to zero. After start-up, at the time $t_2 = 0.4$ s and $t_3 = 0.6$ s nominal load torque is switched on and off to the drive system. Finally, at the time $t_4 = 1$ s the reference value changes to -0.2 . At the beginning, the system with $R = 1$ is tested.

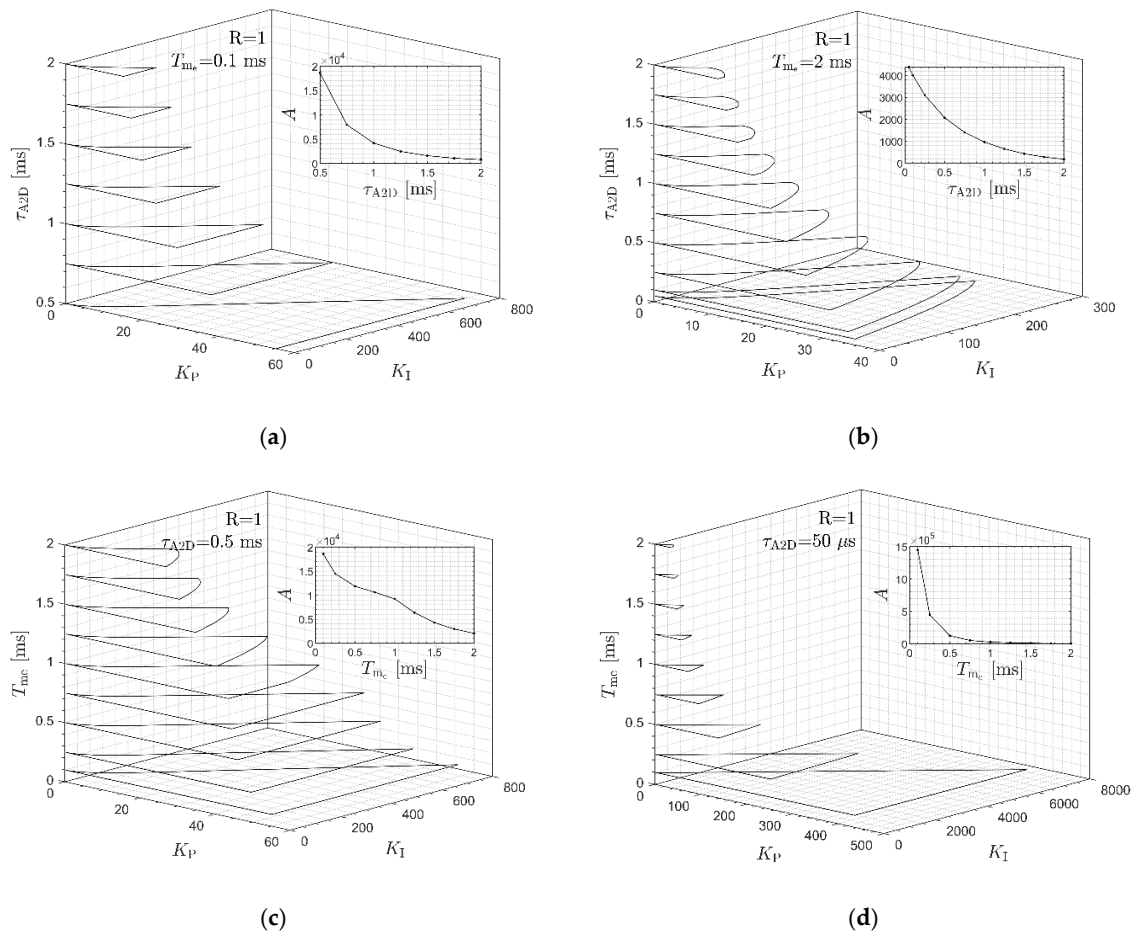


Figure 10. Visualisation of the K_P and K_I regions for desired values of $GM = 20$ dB and $PM = 70^\circ$ for the control structure from Figure 2 calculated using D-decomposition technique. Results were obtained for the value of inertia ratio $R = 1$, time constant of the elastic shaft, $T_C = 2.6$ ms, and value of electromagnetic torque time constant $T_{m_e} = 0.1$ ms (a) and $T_{m_e} = 2$ ms (b) and delay from analog-to-digital conversion in the speed sensor $\tau_{A2D} = 0.5$ ms (c) and $\tau_{A2D} = 50$ μ s (d). Additionally, the total area, A , of obtained regions was presented.



Figure 11. The picture of the experimental set-up: without (a) and with (b) additional flywheel.

Firstly, the system with an IP controller with the coefficients set with the use of the classical method (6) is tested (point P_1 in Figure 7). Next, the system with increased value of the PM is considered (related to point P_2). The obtained transients are recorded. Finally, the control structure with final parameters of the speed controller (point P_3) is considered. In order to compare the characteristics saved for different operation points, transients of particular variable for different operation points are placed in one graph (Figure 12).

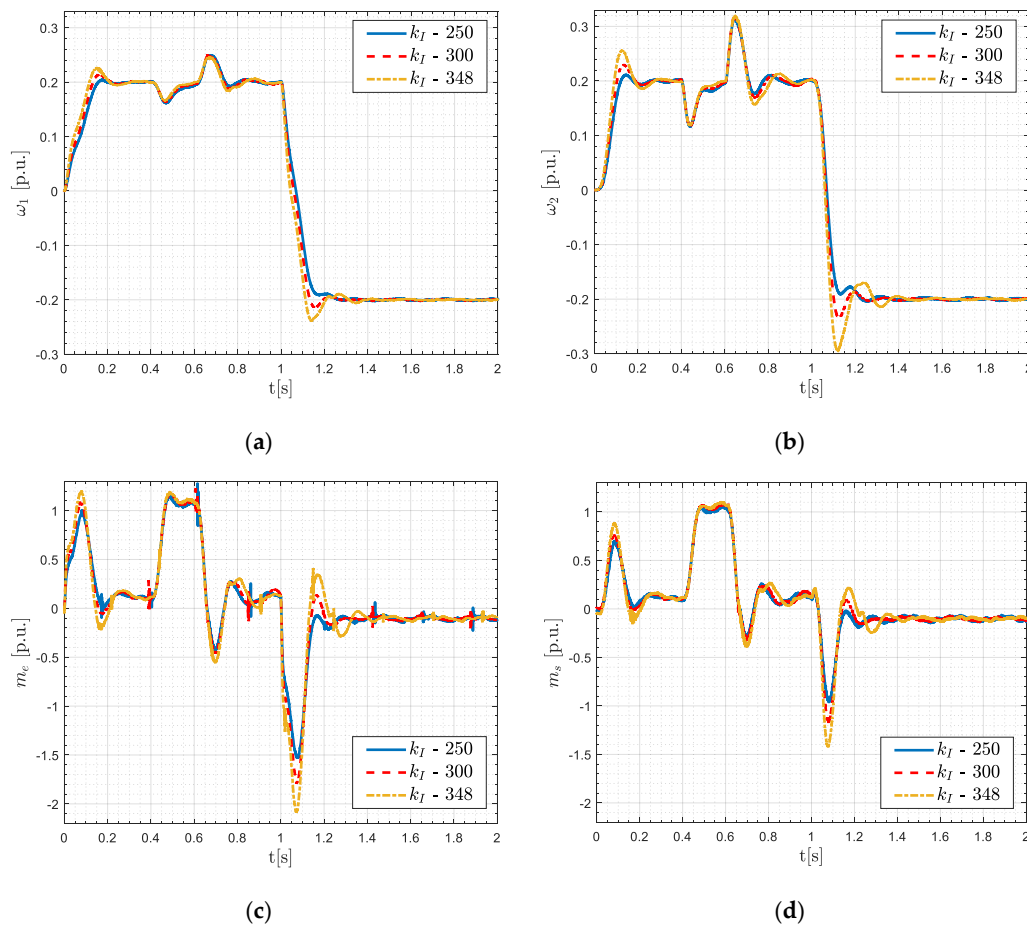


Figure 12. Experimental transients of the two-mass system: motor speed (a), load speed (b), electromagnetic torque, (c) and shaft torque (d) for different gains of the speed controller and value of the reference signal equal to 0.2 for $R = 1$.

The saved experimental transients are presented in Figure 12 in following order. As first transients of driving motor speed (Figure 12a) and load speed (Figure 12b) are placed. Then the electromagnetic (Figure 12c) as well as shaft torque are presented (Figure 12d). The following remarks can be formulated with the help of the mentioned graph. The decrease of the PM lower the overshoot and settling time of the system speeds. The overshoot in load speed is reduced from 28 to 6%. Additionally, the oscillations into torque transients are the smallest for the final point of the works. However, it should be stated that the improvement of the system characteristic for the inertia ratio is not so visible.

Then the system with $R = 0.25$ is tested experimentally. In order to obtain such value of inertia coefficient, an additional flywheel has been added to the motor site. The cycle of work is similar as in the previous considered case. The obtained transients are shown in Figure 13.

As can be concluded from the presented transients the system is working correctly. For the controller tuned with the help of the classical pole-placement methodology (P_1) both speeds possesses large overshoot and settling time (Figure 13a,b—yellow line). Additionally, big oscillations are visible in the electromagnetic and shaft torques transients (Figure 13c,d—yellow line). It should be stressed that in this case, the electromagnetic torque is slightly limited (Figure 13c) which results of reducing overshoots. These features result from the classical poles-placement methodology which guarantee double location of the system closed-loop poles. Because these performances are not acceptable in many practical applications, then D-decomposition technique is proposed to improve the system features. The transients saved for operation point P_2 (red line) and point P_3 (blue line) are presented in Figure 13.

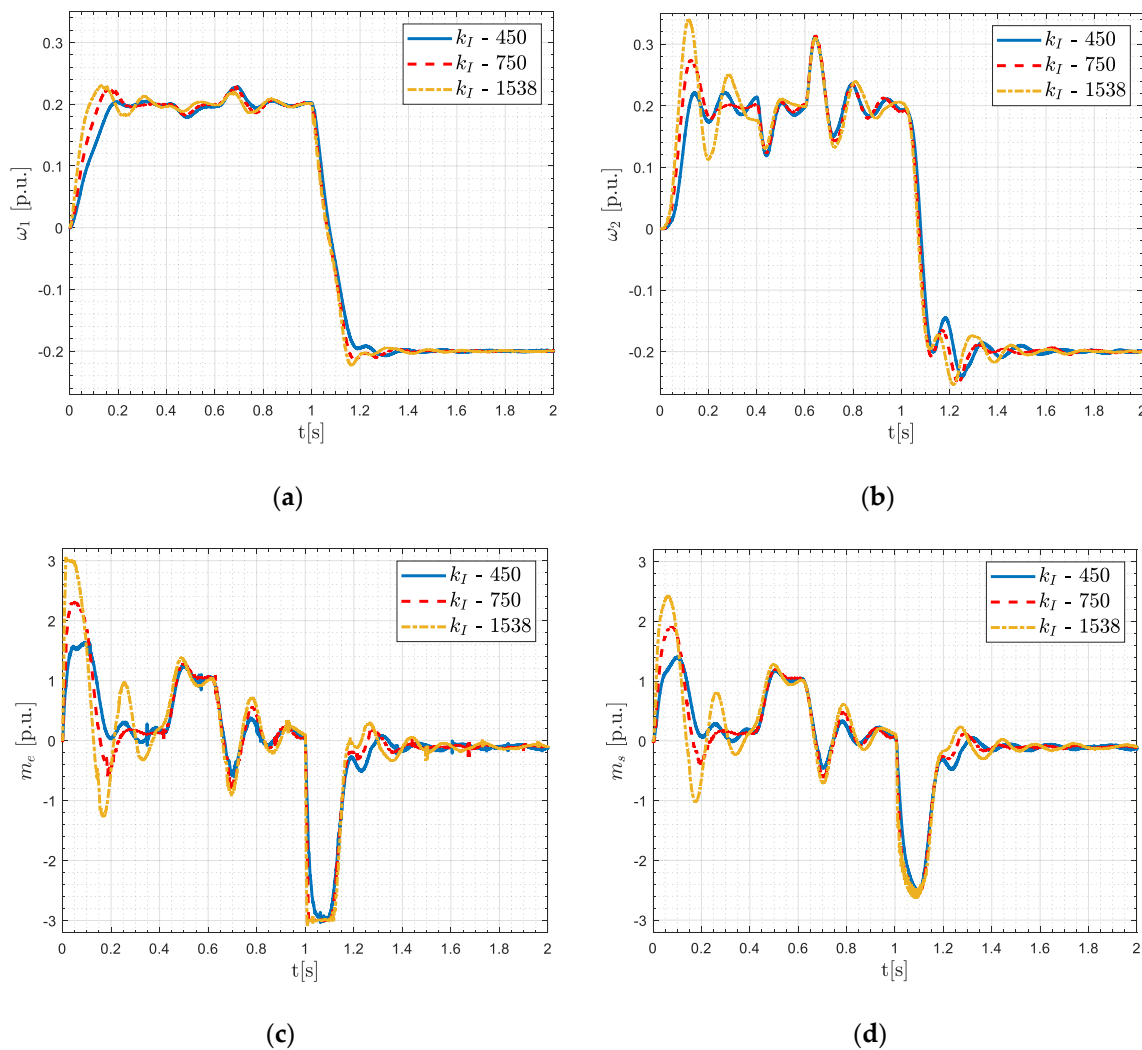


Figure 13. Experimental transients of the two-mass system: motor speed (a), load speed (b), electromagnetic torque (c), and shaft torque (d) for different gains of the speed controller and value of the reference signal equal to 0.2 for $R = 0.25$.

As in the simulation study, the final point ensures the most optimal characteristics of the system. The overshoots of the driving motor and load velocities are reduced significantly (in load speed from 70 to 10%). Additionally, the oscillations of the electromagnetic and shaft torques are much smaller as compared to the previously considered cases. This confirms the effectiveness of the proposed methodology, especially for the system with a small inertia ratio R .

In order to analyze the obtained transients (Figures 12 and 13) more accurately the characteristic values such as rising time, time to first maximum, settling time, overshoot, and others for different working points (P_1, P_2, P_3) and inertia ratio R are calculated. The results are presented in Table 1.

The values presented in Table 1 confirm the previously presented analysis. The systems with working point P_3 have oscillatory responses. The overshoots in both speeds are very large. Additionally, the maximal values of the electromagnetic and shaft torques are the biggest. The changing of working points improve the system performances. The overshoots are reduced significantly as well as the maximal values of torques. The values of settling times are decreases.

Table 1. Characteristic values of the transients for system with $R = 1$ and $R = 0.25$.

		$R = 1$			$R = 0.25$		
		P_1	P_2	P_3	P_1	P_2	P_3
$\delta_{\omega 1}$	[%]	13	7	2	15	12	2
$t_m^{\omega 1}$	[s]	0.15	0.165	0.175	0.13	0.16	0.195
$t_{s2\%}^{\omega 1}$	[s]	0.27	0.204	0.175	0.26	0.25	0.24
$t_r^{\omega 1}$	[s]	0.092	0.103	0.116	0.057	0.087	0.126
$t_{s5\%}^{\omega 1}$	[s]	0.19	0.18	0.142	0.245	0.172	0.154
$\delta_{\omega 2}$	[%]	28	15	6	70	35	10
$t_m^{\omega 2}$	[s]	0.125	0.135	0.145	0.118	0.126	0.14
$t_{s2\%}^{\omega 2}$	[s]	0.4	0.22	0.195	>0.4	>0.4	>0.4
$t_r^{\omega 2}$	[s]	0.047	0.054	0.062	0.036	0.043	0.058
$t_{s5\%}^{\omega 2}$	[s]	0.32	0.207	0.16	>0.4	0.23	>0.4
m_e^{\max}	[p.u.]	1.2	1.08	1	3	2.32	1.63
m_s^{\max}	[p.u.]	0.89	0.76	0.7	2.44	1.91	1.4

Where: $\delta_{\omega x}$ —overshoot of speed, $t_m^{\omega x}$ —time to first maximum of speed, $t_{s2\%}^{\omega x}$, $t_{s5\%}^{\omega x}$ —2% and 5% settling time of speed, $t_r^{\omega x}$ —rising time, m_e^{\max} —maximum value of the electromagnetic torque. m_s^{\max} —maximum value of the shaft torque.

5. Conclusions

The application of the D-decomposition methodology for determination of the control parameters for the drive system with a flexible connection is demonstrated in this work. The classical two-mass drive system with only basic feedback from the driving motor speed is a demanding plant to control. Especially for the small value of inertia ratio R , in motor and load speeds large oscillations are generated. In order to damp those oscillations different control concepts can be used. Usually, advanced control structures based on additional feedback(s) are proposed. However, in many industrial cases simple methodology is required which allows to improve the drive performance without modifying the existing structure. For these situations, the D-decomposition is proposed in this work. Regarding the theoretical considerations and results of the tests, the following concluding remarks can be formulated.

The stable regions of work can be determined with the help of the D-decomposition technique. The designer can assume the values of the phase and gain margins and D-decomposition technique will determine the parameters of the controller. The selection of optimal value of the gain and phase margins for two-mass drive system requires some expertise. Therefore the initial point is calculated with the help of a formula resulting from classical poles-placement methodology. The procedure can be presented in a few steps. First, the classical equations which ensure double location of the system closed-loop poles are used. The obtained results are not optimal—there is a large overshoot in a load speed (especially for a system with small value of R). Then, phase margin is increased until the overshoot in the load speed is reduced to an acceptable value. This also improves transients of the other state variables of the system, such as motor speed as well as electromagnetic and shaft torques. The D-decomposition technique can be used to determine the stable working region of the system taking into account the delay caused by the torque control loop. The obtained area is determined as a function of the controller parameters. Additionally, the influence of the delay in the speed measurement loop can be taken into account. The proposed method is especially effective in the system with a small value of the inertia ratio R . For instance, for the system with $R = 0.25$ the overshoot in the load machine speed is reduced from 70 to 10%. Additionally, the oscillations in other drive states are also suppressed successfully.

The future work will be devoted to formulate general guidelines based on the PM and GM for the two-mass drive system with different values of inertia ratio and resonant frequency as well as

changeable parameters. Additionally, the analysis of the system with an additional feedback (from e.g., shaft torque) will be done.

Author Contributions: All authors contributed equally to this paper, in particular: conceptualization, R.N. and K.S.; methodology, R.N. and K.S.; software, R.N. and K.N.; validation, K.N. and K.W.; formal analysis, R.N., K.N. and K.W.; investigation, K.N. and K.W.; resources, R.N., K.N., K.W. and K.S.; data curation, K.N. and K.W.; writing—original draft preparation, R.N., K.N., K.W. and K.S.; writing—review and editing, R.N. and K.S.; visualization, K.N. and K.W.; supervision, R.N. and K.S.; project administration K.S.; funding acquisition, K.S. All authors have read and agreed to the published version of the manuscript.

Funding: This research received no external funding.

Conflicts of Interest: The authors declare no conflict of interest.

References

1. Katsura, S.; Ohnishi, K. Force servoing by flexible manipulator based on resonance ratio control. *IEEE Trans. Ind. Electron.* **2007**, *54*, 539–547. [\[CrossRef\]](#)
2. Kobayashi, H.; Katsura, S.; Ohnishi, K. An analysis of parameter variations of disturbance observer for motion control. *IEEE Trans. Ind. Electron.* **2007**, *54*, 3413–3421. [\[CrossRef\]](#)
3. Ohnishi, K.; Katsura, S.; Shimono, T. Motion control for real-world haptics. *IEEE Ind. Electron. Mag.* **2010**, *4*, 16–19. [\[CrossRef\]](#)
4. Katsura, S.; Suzuki, J.; Ohnishi, K. Pushing operation by flexible manipulator taking environmental information into account. *IEEE Trans. Ind. Electron.* **2006**, *53*, 1688–1697. [\[CrossRef\]](#)
5. Szabat, K.; Tokarczyk, A.; Wróbel, K.; Katsura, S. Application of the multi-layer observer for a two-mass drive system. In Proceedings of the IEEE 29th International Symposium on Industrial Electronics (ISIE), Delft, The Netherlands, 17–19 June 2020; pp. 265–270.
6. Zhang, G.; Furusho, J. Speed control of two-inertia system by PI/PID Control. *IEEE Trans. Ind. Electron.* **2000**, *47*, 603–609. [\[CrossRef\]](#)
7. Goubey, M. Fundamental performance limitations in PID controlled elastic two-mass systems. In Proceedings of the 2016 IEEE International Conference on Advanced Intelligent Mechatronics (AIM), Banff, AB, Canada, 12–15 July 2016; pp. 828–833.
8. Szabat, K.; Orłowska-Kowalska, T. Vibration suppression in two-mass drive system using PI speed controller and additional feedbacks—Comparative study. *IEEE Trans. Ind. Electron.* **2007**, *54*, 1193–1206. [\[CrossRef\]](#)
9. Serkies, P.; Szabat, K. Effective damping of the torsional vibrations of the drive system with an elastic joint based on the forced dynamic control algorithms. *J. Vib. Control* **2019**, *25*, 2225–2236. [\[CrossRef\]](#)
10. Pakdelian, S.; Moosavi, M.; Hussain, H.A.; Toliyat, H.A. Control of an electric machine integrated with the trans-rotary magnetic gear in a motor drive train. *IEEE Trans. Ind. Appl.* **2017**, *53*, 106–114. [\[CrossRef\]](#)
11. De Pinto, S.; Camocardi, P.; Sornioti, A.; Gruber, P.; Perlo, P.; Viotto, F. Torque-fill control and energy management for a four-wheel-drive electric vehicle layout with two-speed transmissions. *IEEE Trans. Ind. Appl.* **2017**, *53*, 447–458. [\[CrossRef\]](#)
12. Bianchi, N.; Bolognani, S.; Carraro, E.; Castiello, M.; Fornasiero, E. Electric vehicle traction based on synchronous reluctance motors. *IEEE Trans. Ind. Appl.* **2019**, *52*, 4762–4769. [\[CrossRef\]](#)
13. Meeus, H.; Verrelst, B.; Moens, D.; Guillaume, P.; Lefeber, D. Experimental study of the shaft penetration factor on the torsional dynamic response of a drive train. *Machines* **2018**, *6*, 31. [\[CrossRef\]](#)
14. Wang, Y.; Da Ronch, A.; Ghandchi Tehrani, M. Adaptive feedforward control for gust-induced aeroelastic vibrations. *Aerospace* **2018**, *5*, 86. [\[CrossRef\]](#)
15. Tran Anh, D.; Nguyen Trong, T. Adaptive controller of the major functions for controlling a drive system with elastic couplings. *Energies* **2018**, *11*, 531. [\[CrossRef\]](#)
16. Wang, Y.; Yu, H.; Yu, J.; Wu, H.; Liu, X. Trajectory tracking of flexible-joint robots actuated by PMSM via a novel smooth switching control strategy. *Appl. Sci.* **2019**, *9*, 4382. [\[CrossRef\]](#)
17. Chaoui, H.; Gueaieb, W.; Biglarbegian, M.; Yagoub, M.C.E. Computationally efficient adaptive type-2 fuzzy control of flexible-joint manipulators. *Robotics* **2013**, *2*, 66–91. [\[CrossRef\]](#)
18. Ju, J.; Zhao, Y.; Zhang, C.; Liu, Y. Vibration suppression of a flexible-joint robot based on parameter identification and fuzzy PID control. *Algorithms* **2018**, *11*, 189. [\[CrossRef\]](#)

19. Qi, L.; Zheng, L.; Bai, X.; Chen, Q.; Chen, J.; Chen, Y. Nonlinear maximum power point tracking control method for wind turbines considering dynamics. *Appl. Sci.* **2020**, *10*, 811. [CrossRef]
20. Song, M.-H.; Pham, X.D.; Vuong, Q.D. Torsional vibration stress and fatigue strength analysis of marine propulsion shafting system based on engine operation patterns. *J. Mar. Sci. Eng.* **2020**, *8*, 613. [CrossRef]
21. Kessai, I.; Benammar, S.; Doghmane, M.Z.; Tee, K.F. Drill bit deformations in rotary drilling systems under large-amplitude stick-slip vibrations. *Appl. Sci.* **2020**, *10*, 6523. [CrossRef]
22. Liu, H.; Cui, S.; Liu, Y.; Ren, Y.; Sun, Y. Design and vibration suppression control of a modular elastic joint. *Sensors* **2018**, *18*, 1869. [CrossRef]
23. Orłowska-Kowalska, T.; Szabat, K. Damping of torsional vibrations in two-mass system using adaptive sliding neuro-fuzzy approach. *IEEE Trans. Ind. Inform.* **2008**, *4*, 47–57. [CrossRef]
24. Szabat, K.; Orłowska-Kowalska, T. Performance improvement of industrial drives with mechanical elasticity using nonlinear adaptive kalman filter. *IEEE Trans. Ind. Electron.* **2008**, *55*, 1075–1084. [CrossRef]
25. Serkies, P. Estimation of state variables of the drive system with elastic joint using moving horizon estimation (MHE). *Bull. Pol. Acad. Sci. Tech. Sci.* **2019**, *67*, 883–892.
26. Szabat, K.; Wróbel, K.; Drózd, K.; Janiszewski, D.; Pajchrowski, T.; Wójcik, A. A fuzzy unscented kalman filter in the adaptive control system of a drive system with a flexible joint. *Energies* **2020**, *13*, 2056. [CrossRef]
27. Orłowska-Kowalska, T.; Kaminski, M. FPGA implementation of the multilayer neural network for the speed estimation of the two-mass drive system. *IEEE Trans. Ind. Inform.* **2011**, *7*, 436–445. [CrossRef]
28. Kamiński, M.; Orłowska-Kowalska, T. Adaptive neural speed controllers applied for a drive system with an elastic mechanical coupling—A comparative study. *Eng. Appl. Artif. Intell.* **2015**, *45*, 152–167. [CrossRef]
29. Brock, S.; Luczak, D.; Nowopolski, K.; Pajchrowski, T.; Zawirski, K. Two approaches to speed control for multi-mass system with variable mechanical parameters. *IEEE Trans. Ind. Electron.* **2016**, *64*, 3338–3347. [CrossRef]
30. Inoue, Y.; Katsura, S. Spatial disturbance suppression of a flexible system based on wave model. *IEEE J. Ind. Appl.* **2018**, *7*, 236–243. [CrossRef]
31. Szczepański, R.; Kamiński, M.; Tarczewski, T. Auto-tuning process of state feedback speed controller applied for two-mass system. *Energies* **2020**, *13*, 3067. [CrossRef]
32. Najdek, K.; Nalepa, K.; Szabat, K. Selection of controller parameters of a two-mass drive system using the d-decomposition technique. In Proceedings of the IECON—45th Annual Conference of the IEEE Industrial Electronics Society, Lisbon, Portugal, 14–17 October 2019; pp. 1308–1313.
33. Nijmark, J.I. Ob opriedielenji znaczenij paramietrow, pri kotorych sistiema awtomaticheskogo riegulirowanja ustojczywa. *Awtomatika Telemekhanika* **1948**, *3*, 190–203.
34. Shenton, A.T.; Shafiei, Z. Relative stability for control systems with adjustable parameters. *J. Guid. Control. Dyn.* **1994**, *17*, 304–310. [CrossRef]
35. Osuský, J.; Veselý, V. Modification of Neimark D-partition method for desired phase margin. International Conference: Cybernetics and Informatics, Vyšná Boca, Slovak Republic, 10–13 February 2010; Volume 10, pp. 1–7.
36. Amariutei, R.-D.; Goras, L.; Dobler, M.; Rafaila, M.; Buzo, A.; Pelz, G. On the stability domain of a DC-DC buck converter with software control loop. In Proceedings of the 19th International Conference on System Theory, Control and Computing (ICSTCC), Cheile Gradistei, Romania, 14–16 October 2015; pp. 811–816.
37. Schlegel, M.; Medvecová, P. Design of PI controllers: H_∞ Region Approach. *IFAC-PapersOnLine* **2018**, *51*, 13–17. [CrossRef]
38. Čech, M.; Miloš Schlegel, M. Fractional-order PID controller design on Internet: www.PIDlab.com. In Proceedings of the 7th International Carpathian Control Conference ICC, Ostrava-Beskydy, Czech Republic, 29–31 May 2006; pp. 1–4.
39. Najdek, K.; Nalepa, R. Use of the D-decomposition technique for gains selection of the Dual Active Bridge converter output voltage regulator. *Przegląd Elektrotechniczny* **2019**, *95*, 268–273. [CrossRef]

Publisher’s Note: MDPI stays neutral with regard to jurisdictional claims in published maps and institutional affiliations.



© 2020 by the authors. Licensee MDPI, Basel, Switzerland. This article is an open access article distributed under the terms and conditions of the Creative Commons Attribution (CC BY) license (<http://creativecommons.org/licenses/by/4.0/>).